The Astrophysical Journal, 739:40 (8pp), 2011 September 20 doi:10.1088/0004-637X/739/1/40

POLARIZED LINE FORMATION IN MULTI-DIMENSIONAL MEDIA. IV. A FOURIER DECOMPOSITION TECHNIQUE TO FORMULATE THE TRANSFER EQUATION WITH ANGLE-DEPENDENT PARTIAL FREQUENCY REDISTRIBUTION

L. S. Anusha and K. N. Nagendra
Indian Institute of Astrophysics, Koramangala, 2nd Block, Bangalore 560 034, India
Received 2011 May 11; accepted 2011 July 6; published 2011 September 6

ABSTRACT

To explain the linear polarization observed in spatially resolved structures in the solar atmosphere, the solution of polarized radiative transfer (RT) equation in multi-dimensional (multi-D) geometries is essential. For strong resonance lines, partial frequency redistribution (PRD) effects also become important. In a series of papers, we have been investigating the nature of Stokes profiles formed in multi-D media including PRD in line scattering. For numerical simplicity, so far we have restricted our attention to the particular case of PRD functions which are averaged over all the incident and scattered directions. In this paper, we formulate the polarized RT equation in multi-D media that takes into account the Hanle effect with angle-dependent PRD functions. We generalize here to the multi-D case the method for Fourier series expansion of angle-dependent PRD functions originally developed for RT in one-dimensional geometry. We show that the Stokes source vector $\boldsymbol{S} = (S_I, S_Q, S_U)^T$ and the Stokes vector $\boldsymbol{I} = (I, Q, U)^T$ can be expanded in terms of infinite sets of components $\tilde{\mathcal{S}}^{(k)}$, $\tilde{\mathcal{I}}^{(k)}$, respectively, $k \in [0, +\infty)$. We show that the components $\tilde{\mathcal{S}}^{(k)}$ become independent of the azimuthal angle (φ) of the scattered ray, whereas the components $\tilde{\mathcal{I}}^{(k)}$ remain dependent on φ due to the nature of RT in multi-D geometry. We also establish that $\tilde{\mathcal{S}}^{(k)}$ and $\tilde{\mathcal{I}}^{(k)}$ satisfy a simple transfer equation, which can be solved by any iterative method such as an approximate Lambda iteration or a Bi-Conjugate Gradient-type projection method provided we truncate the Fourier series to have a finite number of terms.

Key words: line: formation – magnetic fields – polarization – radiative transfer – scattering – Sun: atmosphere

1. INTRODUCTION

Observations of the solar atmosphere reveal a wealth of information about the spatially inhomogeneous structures. Modern spectropolarimeters with high spatial and polarimetric resolution are able to distinguish the changes in the linearly polarized spectrum caused by such structures. To model the spectropolarimetric observations of such spatially resolved structures, one has to solve a three-dimensional (3D) polarized line radiative transfer (RT) equation. A historical account of the developments of RT in multi-dimensional (multi-D) media is presented in detail in Anusha & Nagendra (2011a, hereafter Paper I). In a series of papers, we have been investigating the nature of linearly polarized profiles formed in multi-D media, taking into account the partial frequency redistribution (PRD) in line scattering. In Paper I, we developed a method for "Stokes vector decomposition" in multi-D geometry in terms of "irreducible spherical tensors" $\mathcal{T}^K_Q$ (see Landi Degl'Innocenti & Landolfi 2004). It was a generalization to the multi-D case, of the decomposition technique developed in Frisch (2007, hereafter HF07) for the one-dimensional (1D) case. In Anusha et al. (2011, hereafter Paper II), we developed a fast numerical method called the Pre-BiCG-STAB (Stabilized preconditioned Bi-Conjugate Gradient), to solve the polarized RT problems in two-dimensional (2D) media. In Anusha & Nagendra (2011b, hereafter Paper III), we generalized the works of Papers I and II to include scattering in the presence of weak magnetic fields (Hanle effect) in a 3D geometry. In all these papers we considered only angle-averaged PRD functions.

The polarized Stokes line transfer problems with angle-dependent PRD in 1D planar geometries were solved by several authors (see Dumont et al. 1977; McKenna 1985; Faurobert 1987, 1988; Nagendra et al. 2002, 2003; Sampoorna et al. 2008). In this formalism, a strong coupling of incident and scattered ray directions ($\boldsymbol{\Omega}'$ and $\boldsymbol{\Omega}$ respectively) prevails in the scattering phase matrices as well as the angle-dependent PRD functions, which brings in unmitigated numerical difficulties. To simplify the problem, a method based on "decomposition of the phase matrices" in terms of $\mathcal{T}^K_Q$ combined with a "Fourier series expansion" of the angle-dependent redistribution functions $r_{\rm II,III}(x, x', \boldsymbol{\Omega}, \boldsymbol{\Omega}')$ of Hummer (1962) was proposed for Hanle and Rayleigh scattering by Frisch (2009, hereafter HF09) and Frisch (2010), respectively. Sampoorna et al. (2011) developed efficient numerical methods to solve angle-dependent RT problems for the case of Rayleigh scattering, based on the decomposition technique developed by Frisch (2010). Sampoorna (2011) proposed a single scattering approximation to solve the more difficult problem of RT with angle-dependent PRD including the Hanle effect. However, all these works are confined to the limit of 1D planar geometry.

In this paper, we generalize to the multi-D case, the Fourier decomposition technique developed in HF09 for the 1D case. In the first step, we decompose the phase matrices in terms of $\mathcal{T}^K_Q$ as done in Papers I and III. However, we now formulate a polarized RT equation for multi-D that also includes angle-dependent PRD functions. We set up a transfer equation in terms of a new set of six-dimensional (6D) vectors called the "irreducible source and the irreducible Stokes vectors." In the second step, we expand the $r_{\rm II,III}(x, x', \boldsymbol{\Omega}, \boldsymbol{\Omega}')$ redistribution functions in terms of a Fourier series with respect to the azimuthal angle (φ) of the scattered ray. Then we transform the original RT equation into a new RT equation, which is simpler to solve because the latter has smaller number of independent variables. This simplified (reduced) transfer equation can be solved by any iterative method such as the approximate Lambda iteration (ALI) or a Bi-Conjugate Gradient-type projection method.

In Table 1 we list the important milestones in the specific area of "formulation and solution of the polarized RT equation"

Table 1
Evolution of Ideas in the Past Three Decades to Simplify the Difficult Problem of Formulating/Solving the Polarized Line Transfer Equation

Milestones	$\boldsymbol{B} = 0$ (Rayleigh Scattering)	$\boldsymbol{B} \neq 0$ (Hanle Effect)
(1) Formulation of PM in Stokes vector formulation	Chandrasekhar (1946) Hamilton (1947)	Stenflo (1978)
(2) Stokes vector RTE: 1D/CRD	Rees (1978)	Faurobert-Scholl (1991) Nagendra et al. (2002)
(3) Stokes vector RTE: multi-D/CRD	Paletou et al. (1999)	
(4) Stokes vector RTE: 1D/PRD	Rees & Saliba (1982): AA Dumont et al. (1977): AD Nagendra (1986): AA Faurobert (1987): AA/AD	Faurobert-Scholl (1991): AA Nagendra et al. (2002): AA/AD
(5) PM decomposition in terms of $\mathcal{T}^K_Q$	Landi Degl'Innocenti & Landi Degl'Innocenti (1988)	Landi Degl'Innocenti & Landi Degl'Innocenti (1988)
(6) Irreducible Stokes source vector in Stokes vector RTE: 1D/CRD	Landi Degl'Innocenti et al. (1987)	Landi Degl'Innocenti et al. (1987)
(7) Irreducible Stokes source vector in Stokes vector RTE: multi-D/CRD	Manso Sainz & Trujillo Bueno (1999) Dittmann (1999)	Manso Sainz & Trujillo Bueno (1999) Dittmann (1999)
(8) Irreducible Stokes vector RTE: 1D/PRD	Frisch (2007)	Frisch (2007)
(9) Formulation of polarized RM:	Omont et al. (1972) Domke & Hubeny (1988)	Omont et al. (1973) Bommier (1997a, 1997b)
(10) RTE with RM: 1D/AA	Faurobert-Scholl (1991) Nagendra (1994)	Nagendra et al. (2002)
(11) RTE with RM: multi-D/AA	Anusha & Nagendra (2011a) Anusha et al. (2011)	Anusha & Nagendra (2011b)
(12) RTE with RM: 1D/AD	Faurobert (1987) Nagendra et al. (2002)	Nagendra et al. (2002) Sampoorna et al. (2008)
(13) Fourier decomposition of AD PRD functions: 1D	Frisch (2009, 2010)	Frisch (2009)
(14) RTE with RM based on Fourier expansions of AD PRD functions: 1D	Sampoorna et al. (2011)	Sampoorna (2011) Nagendra & Sampoorna (2011)
(15) a. RTE with RM: multi-D/AD b. Fourier expansion of AD PRD functions: multi-D c. RTE with RM based on Fourier expansions of AD PRD functions: multi-D	Present paper and Forthcoming paper	Present paper and Forthcoming paper

Notes. RTE: radiative transfer equation; AA: angle-averaged; AD: angle-dependent; PM: phase matrix; RM: redistribution matrix; CRD: complete frequency redistribution; PRD: partial frequency redistribution.

with resonance scattering and/or Hanle effect in 1D and multi-D media in different formalisms. The emphasis is on showing how the complexity of the problem is reduced to manageable levels by the concerted efforts of several authors. It includes a brief historical account of the formulation and decomposition of polarized phase matrices and the redistribution matrices for spectral lines. In the literature on this topic, the term "phase matrix" refers only to the angular correlations in the polarized light scattering (see, e.g., the Rayleigh scattering polarized phase matrix described in Chandrasekhar 1960). The phase matrices are, in general, frequency independent. The "redistribution matrix," on the other hand, contains both frequency and angle correlations between the incident and scattered photons. The formulation of the redistribution matrices in the astrophysical literature (in the modern analytic form) dates back to the pioneering work of Omont et al. (1972, 1973). The references given here serve only to mark the milestones. No pretension is made to give a full list of references.

In Section 2, we describe the multi-D transfer equation in the Stokes vector formalism. An irreducible transfer equation for angle-dependent PRD functions in multi-D media is presented in Section 3. In Section 4, a transfer equation in multi-D geometry for the irreducible Fourier coefficients of the Stokes source vector and the Stokes vector is established. Conclusions are given in Section 6.

2. TRANSFER EQUATION IN TERMS OF STOKES PARAMETERS

For a given ray defined by the direction $\boldsymbol{\Omega}$, the polarized transfer equation in a multi-D medium for a two-level model

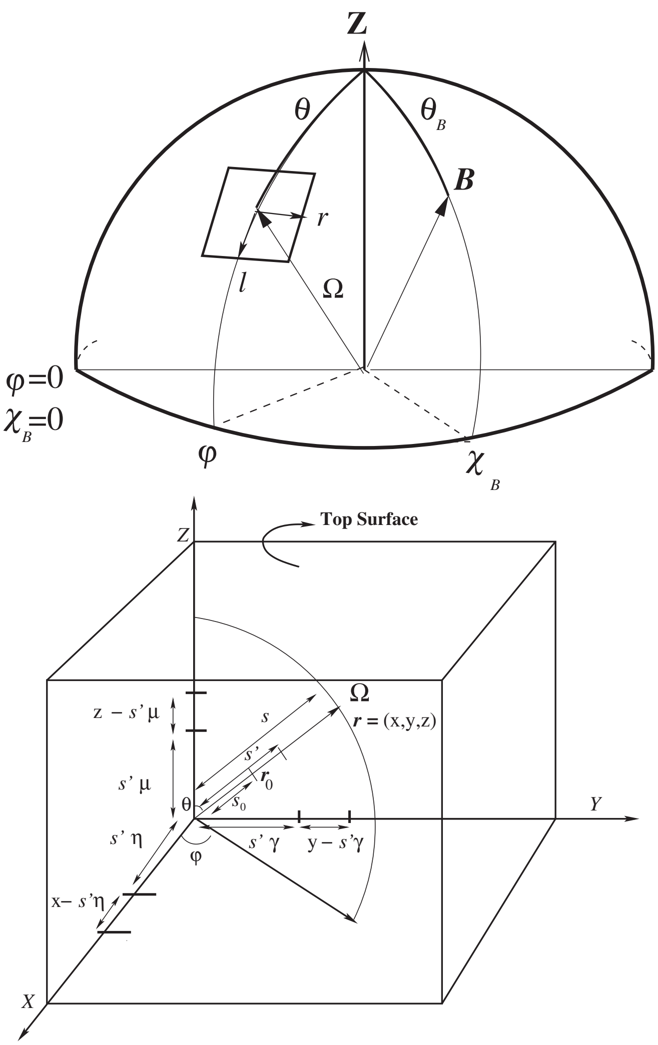

Figure 1. Top: the atmospheric reference frame. The angle pair (θ, φ) defines the scattered ray direction. The magnetic field is characterized by $\boldsymbol{B} = (\Gamma, \theta_B, \chi_B)$, where Γ is the Hanle efficiency parameter and (θ_B, χ_B) define the field direction. Bottom: the definition of the position vector $\boldsymbol{r}$ and the projected distances $\boldsymbol{r} - s'\boldsymbol{\Omega}$ which appear in Equation (6). Here, $\boldsymbol{r}_0$ and $\boldsymbol{r}$ are the arbitrary initial and final locations that appear in the formal solution integral (Equation (6)).

atom with unpolarized ground level is given by

$$\boldsymbol{\Omega} \cdot \nabla \boldsymbol{I}(\boldsymbol{r}, \boldsymbol{\Omega}, x) = -[\kappa_l(\boldsymbol{r})\phi(x) + \kappa_c(\boldsymbol{r})] \times [\boldsymbol{I}(\boldsymbol{r}, \boldsymbol{\Omega}, x) - \boldsymbol{S}(\boldsymbol{r}, \boldsymbol{\Omega}, x)]. \quad (1)$$

Equations analogous to Equation (1) for the unpolarized case can be found in several references (see, e.g., Adam 1990; Mihalas et al. 1978; Pomraning 1973). For the polarized case with PRD, the transfer equations are given in Papers I–III. Here, $\boldsymbol{I} = (I, Q, U)^T$ is the Stokes vector with I, Q, and U being the Stokes parameters defined as in Chandrasekhar (1960). The reference directions l and r are marked in the top panel of Figure 1. The positive value of Q is defined to be in a direction parallel to l and negative Q in a direction parallel to r. The quantity $\boldsymbol{r} = (\mathrm{x}, \mathrm{y}, \mathrm{z})$ is the position vector of the ray in the Cartesian coordinate system (see the bottom panel of Figure 1). The unit vector $\boldsymbol{\Omega} = (\eta, \gamma, \mu) = (\sin\theta \cos\varphi, \sin\theta \sin\varphi, \cos\theta)$ defines the direction cosines of the ray in the atmosphere with respect to the atmospheric normal (the Z-axis), where θ and φ are the polar and azimuthal angles of the ray, respectively (see Figure 1).

The quantity κ_l is the frequency-averaged line opacity, ϕ is the Voigt profile function, and κ_c is the continuum opacity. Frequency is measured in reduced units, namely $x = (\nu - \nu_0)/\Delta\nu_D$, where $\Delta\nu_D$ is the Doppler width. The Stokes source vector in a two-level model atom with unpolarized ground level (see, e.g., Faurobert 1987; Nagendra et al. 2002) is

$$\boldsymbol{S}(\boldsymbol{r}, \boldsymbol{\Omega}, x) = \frac{\kappa_l(\boldsymbol{r})\phi(x)\boldsymbol{S}_l(\boldsymbol{r}, \boldsymbol{\Omega}, x) + \kappa_c(\boldsymbol{r})\boldsymbol{S}_c(\boldsymbol{r}, x)}{\kappa_l(\boldsymbol{r})\phi(x) + \kappa_c(\boldsymbol{r})}. \quad (2)$$

Here, $\boldsymbol{S}_c$ is the unpolarized continuum source vector given by $(B_\nu(\boldsymbol{r}), 0, 0)^T$, with $B_\nu(\boldsymbol{r})$ being the Planck function. The line source vector (see, e.g., Faurobert 1987; Nagendra et al. 2002) is written as

$$\boldsymbol{S}_l(\boldsymbol{r}, \boldsymbol{\Omega}, x) = \boldsymbol{G}(\boldsymbol{r}) + \int_{-\infty}^{+\infty} dx' \oint \frac{d\boldsymbol{\Omega}'}{4\pi} \times \frac{\hat{R}(x, x', \boldsymbol{\Omega}, \boldsymbol{\Omega}', \boldsymbol{B})}{\phi(x)} \boldsymbol{I}(\boldsymbol{r}, \boldsymbol{\Omega}', x'). \quad (3)$$

Here, $\hat{R}$ is the Hanle redistribution matrix with angle-dependent PRD (see Section 4.2, approximation level II of Bommier 1997b); $\boldsymbol{B}$ represents an oriented vector magnetic field. The thermalization parameter $\epsilon = \Gamma_I/(\Gamma_R + \Gamma_I)$, with Γ_I and Γ_R being the inelastic collision rate and the radiative de-excitation rate, respectively. The damping parameter is computed using $a = a_R[1 + (\Gamma_E + \Gamma_I)/\Gamma_R]$, where $a_R = \Gamma_R/4\pi\Delta\nu_D$ and Γ_E is the elastic collision rate. We denote the thermal source vector by $\boldsymbol{G}(\boldsymbol{r}) = \epsilon\boldsymbol{B}_\nu(\boldsymbol{r})$ with $\boldsymbol{B}_\nu(\boldsymbol{r}) = (B_\nu(\boldsymbol{r}), 0, 0)^T$. The solid angle element $d\boldsymbol{\Omega}' = \sin\theta'\, d\theta'\, d\varphi'$, where $\theta \in [0, \pi]$ and $\varphi \in [0, 2\pi]$. The transfer equation along the ray path takes the form

$$\frac{d\boldsymbol{I}(\boldsymbol{r}, \boldsymbol{\Omega}, x)}{ds} = -\kappa_{\mathrm{tot}}(\boldsymbol{r}, x)[\boldsymbol{I}(\boldsymbol{r}, \boldsymbol{\Omega}, x) - \boldsymbol{S}(\boldsymbol{r}, \boldsymbol{\Omega}, x)], \quad (4)$$

where s is the path length along the ray and $\kappa_{\mathrm{tot}}(\boldsymbol{r}, x)$ is the total opacity given by

$$\kappa_{\mathrm{tot}}(\boldsymbol{r}, x) = \kappa_l(\boldsymbol{r})\phi(x) + \kappa_c(\boldsymbol{r}). \quad (5)$$

The formal solution of Equation (4) is given by

$$\boldsymbol{I}(\boldsymbol{r}, \boldsymbol{\Omega}, x) = \boldsymbol{I}(\boldsymbol{r}_0, \boldsymbol{\Omega}, x) \exp\left\{-\int_{s_0}^{s} \kappa_{\mathrm{tot}}(\boldsymbol{r} - s''\boldsymbol{\Omega}, x)\, ds''\right\} + \int_{s_0}^{s} \boldsymbol{S}(\boldsymbol{r} - s'\boldsymbol{\Omega}, \boldsymbol{\Omega}, x)\kappa_{\mathrm{tot}}(\boldsymbol{r} - s'\boldsymbol{\Omega}, x) \times \exp\left\{-\int_{s'}^{s} \kappa_{\mathrm{tot}}(\boldsymbol{r} - s''\boldsymbol{\Omega}, x)\, ds''\right\} ds', \quad (6)$$

where $\boldsymbol{I}(\boldsymbol{r}_0, \boldsymbol{\Omega}, x)$ is the boundary condition imposed at $\boldsymbol{r}_0 = (\mathrm{x}_0, \mathrm{y}_0, \mathrm{z}_0)$. Here, s is the distance measured along the ray path (see the bottom panel of Figure 1). Equations (1)–(6) can be solved using a perturbation method (see Nagendra et al. 2002, for the corresponding 1D case). However, the perturbation method involves an approximation that the degree of linear polarization is small (only a few percent). Where the degree of polarization becomes large, the perturbation method cannot be expected to guarantee a stable solution. A numerical disadvantage of working in Stokes vector formalism is that the physical quantities depend on all the angular variables $(\boldsymbol{\Omega}, \boldsymbol{\Omega}')$. Added to this, the angle-dependent polarized RT problem demands high angular grid resolution, thereby requiring enormous memory and CPU time.

3. TRANSFER EQUATION IN TERMS OF IRREDUCIBLE SPHERICAL TENSORS

As shown in HF07, $\boldsymbol{S}$ and $\boldsymbol{I}$ can be decomposed into 6D cylindrically symmetrical vectors $\boldsymbol{\mathcal{S}}$ and $\boldsymbol{\mathcal{I}}$ defined for a 1D geometry as

$$\boldsymbol{\mathcal{S}} = \left(S_0^0, S_0^2, S_1^{2,\mathrm{x}}, S_1^{2,\mathrm{y}}, S_2^{2,\mathrm{x}}, S_2^{2,\mathrm{y}}\right)^T,$$
$$\boldsymbol{\mathcal{I}} = \left(I_0^0, I_0^2, I_1^{2,\mathrm{x}}, I_1^{2,\mathrm{y}}, I_2^{2,\mathrm{x}}, I_2^{2,\mathrm{y}}\right)^T. \quad (7)$$

In Papers I and III, generalizations of the technique of HF07 to the multi-D case are discussed for the case of angle-averaged PRD. We show here that the same decomposition method can be applied to the corresponding angle-dependent PRD case by replacing the angle-averaged PRD functions with angle-dependent PRD functions. This leads to an additional dependence of $\boldsymbol{\mathcal{S}}$ on the scattered ray direction $\boldsymbol{\Omega}$. The vectors $\boldsymbol{\mathcal{I}}$ and $\boldsymbol{\mathcal{S}}$ satisfy a transfer equation of the form

$$-\frac{1}{\kappa_{\mathrm{tot}}(\boldsymbol{r}, x)}\boldsymbol{\Omega}\cdot\nabla\boldsymbol{\mathcal{I}}(\boldsymbol{r}, \boldsymbol{\Omega}, x) = [\boldsymbol{\mathcal{I}}(\boldsymbol{r}, \boldsymbol{\Omega}, x) - \boldsymbol{\mathcal{S}}(\boldsymbol{r}, \boldsymbol{\Omega}, x)], \quad (8)$$

where

$$\boldsymbol{\mathcal{S}}(\boldsymbol{r}, \boldsymbol{\Omega}, x) = p_x \boldsymbol{\mathcal{S}}_l(\boldsymbol{r}, \boldsymbol{\Omega}, x) + (1 - p_x)\boldsymbol{\mathcal{S}}_C(\boldsymbol{r}, x) \quad (9)$$

and

$$p_x = \kappa_l(\boldsymbol{r})\phi(x)/\kappa_{\mathrm{tot}}(\boldsymbol{r}, x). \quad (10)$$

The irreducible line source vector is given by

$$\boldsymbol{\mathcal{S}}_l(\boldsymbol{r}, \boldsymbol{\Omega}, x) = \boldsymbol{G}(\boldsymbol{r}) + \frac{1}{\phi(x)}\int_{-\infty}^{+\infty} dx' \times \oint \frac{d\boldsymbol{\Omega}'}{4\pi}\hat{W}\{\hat{M}_{\mathrm{II}}(\boldsymbol{B}, x, x')r_{\mathrm{II}}(x, x', \boldsymbol{\Omega}, \boldsymbol{\Omega}') + \hat{M}_{\mathrm{III}}(\boldsymbol{B}, x, x')r_{\mathrm{III}}(x, x', \boldsymbol{\Omega}, \boldsymbol{\Omega}')\}\hat{\Psi}(\boldsymbol{\Omega}') \times \boldsymbol{\mathcal{I}}(\boldsymbol{r}, \boldsymbol{\Omega}', x'), \quad (11)$$

with $\boldsymbol{G}(\boldsymbol{r}) = (\epsilon \boldsymbol{B}_\nu(\boldsymbol{r}), 0, 0, 0, 0, 0)^T$ and the irreducible unpolarized continuum source vector $\boldsymbol{\mathcal{S}}_C(\boldsymbol{r}, x) = (S_C(\boldsymbol{r}, x), 0, 0, 0, 0, 0)^T$. We assume that $S_C(\boldsymbol{r}, x) = B_\nu(\boldsymbol{r})$. Here, $\hat{W}$ is a diagonal matrix written as

$$\hat{W} = \mathrm{diag}\{W_0, W_2, W_2, W_2, W_2, W_2\}. \quad (12)$$

Note that $r_{\mathrm{II,III}}$ are the well-known angle-dependent PRD functions of Hummer (1962), which depend explicitly on the scattering angle Θ, defined through $\cos\Theta = \boldsymbol{\Omega}\cdot\boldsymbol{\Omega}'$ computed using

$$\cos\Theta = \mu\mu' + \sqrt{(1-\mu^2)(1-\mu'^2)}\cos(\varphi' - \varphi). \quad (13)$$

The matrix $\hat{\Psi}$ represents the reduced phase matrix for the Rayleigh scattering. Its elements are listed in Appendix D of Paper III. The elements of the matrices $\hat{M}_{\mathrm{II,III}}(\boldsymbol{B}, x, x')$ can be found in Bommier (1997b). The formal solution now takes the form

$$\boldsymbol{\mathcal{I}}(\boldsymbol{r}, \boldsymbol{\Omega}, x) = \boldsymbol{\mathcal{I}}(\boldsymbol{r}_0, \boldsymbol{\Omega}, x)e^{-\tau_{x,\max}} + \int_0^{\tau_{x,\max}} e^{-\tau_x'(\boldsymbol{r}')}\boldsymbol{\mathcal{S}}(\boldsymbol{r}', \boldsymbol{\Omega}, x)\,d\tau_x'(\boldsymbol{r}'). \quad (14)$$

Here, $\boldsymbol{\mathcal{I}}(\boldsymbol{r}_0, \boldsymbol{\Omega}, x)$ is the boundary condition imposed at $\boldsymbol{r}_0$. The monochromatic optical depth scale is defined as

$$\tau_x(\mathrm{x}, \mathrm{y}, \mathrm{z}) = \int_{s_0}^{s} \kappa_{\mathrm{tot}}(\boldsymbol{r} - s''\boldsymbol{\Omega}, x)\,ds'', \quad (15)$$

where τ_x is measured along a given ray determined by the direction $\boldsymbol{\Omega}$. In Equation (14), $\tau_{x,\max}$ is the maximum monochromatic optical depth at frequency x when measured along the ray.

One can develop iterative methods to solve Equations (8)–(14). Because the physical quantities (e.g., $\boldsymbol{\mathcal{S}}$) still depend on $\boldsymbol{\Omega}$, it is not numerically very efficient. In the next section, we present a method to transform Equation (8) into a new RT equation, which is simpler to solve.

4. TRANSFER EQUATION IN TERMS OF IRREDUCIBLE FOURIER COEFFICIENTS

HF09 introduced a method for Fourier series expansion of the angle-dependent PRD functions $r_{\mathrm{II,III}}(x, x', \boldsymbol{\Omega}, \boldsymbol{\Omega}')$. Here we present a generalization to the multi-D case, the formulation given in HF09.

Theorem: In a multi-D polarized RT including angle-dependent PRD and Hanle effect, the irreducible source vector $\boldsymbol{\mathcal{S}}$ and the irreducible Stokes vector $\boldsymbol{\mathcal{I}}$ exhibit Fourier expansions of the form

$$\boldsymbol{\mathcal{S}}(\boldsymbol{r}, \boldsymbol{\Omega}, x) = \sum_{k=-\infty}^{k=\infty} e^{ik\varphi}\,\tilde{\boldsymbol{\mathcal{S}}}^{(k)}(\boldsymbol{r}, \theta, x),$$
$$\boldsymbol{\mathcal{I}}(\boldsymbol{r}, \boldsymbol{\Omega}, x) = \sum_{k=-\infty}^{k=\infty} e^{ik\varphi}\,\tilde{\boldsymbol{\mathcal{I}}}^{(k)}(\boldsymbol{r}, \boldsymbol{\Omega}, x), \quad (16)$$

and that the Fourier coefficients $\tilde{\boldsymbol{\mathcal{S}}}^{(k)}$ and $\tilde{\boldsymbol{\mathcal{I}}}^{(k)}$ satisfy a transfer equation of the form

$$-\frac{1}{\kappa_{\mathrm{tot}}(\boldsymbol{r}, x)}\boldsymbol{\Omega}\cdot\nabla\tilde{\boldsymbol{\mathcal{I}}}^{(k)}(\boldsymbol{r}, \boldsymbol{\Omega}, x) = [\tilde{\boldsymbol{\mathcal{I}}}^{(k)}(\boldsymbol{r}, \boldsymbol{\Omega}, x) - \tilde{\boldsymbol{\mathcal{S}}}^{(k)}(\boldsymbol{r}, \theta, x)]. \quad (17)$$

Proof: The proof is given for the general case of a frequency domain-based PRD (approximation level II) which was derived by Bommier (1997a, 1997b). Since the angle-dependent PRD functions $r_{\mathrm{II,III}}(x, x', \boldsymbol{\Omega}, \boldsymbol{\Omega}')$ are periodic functions of φ with a period 2π, we can express them in terms of a Fourier series

$$r_{\mathrm{II,III}}(x, x', \boldsymbol{\Omega}, \boldsymbol{\Omega}') = \sum_{k=-\infty}^{k=\infty} e^{ik\varphi}\,\tilde{r}^{(k)}_{\mathrm{II,III}}(x, x', \theta, \boldsymbol{\Omega}'), \quad (18)$$

where the Fourier coefficients $\tilde{r}^{(k)}_{\mathrm{II,III}}$ are given by

$$\tilde{r}^{(k)}_{\mathrm{II,III}}(x, x', \theta, \boldsymbol{\Omega}') = \int_0^{2\pi}\frac{d\varphi}{2\pi}\,e^{-ik\varphi}\,r_{\mathrm{II,III}}(x, x', \boldsymbol{\Omega}, \boldsymbol{\Omega}'). \quad (19)$$

We let

$$\boldsymbol{G}(\boldsymbol{r}) = \sum_{k=-\infty}^{k=\infty} e^{ik\varphi}\,\tilde{\boldsymbol{G}}^{(k)}(\boldsymbol{r}), \quad (20)$$

where

$$\tilde{\boldsymbol{G}}^{(k)}(\boldsymbol{r}) = \int_0^{2\pi}\frac{d\varphi}{2\pi}\,e^{-ik\varphi}\,\boldsymbol{G}(\boldsymbol{r}). \quad (21)$$

Note that

$$\tilde{\boldsymbol{G}}^{(k)}(\boldsymbol{r}) = \begin{cases} \boldsymbol{G}(\boldsymbol{r}) & \text{if } k = 0, \\ 0 & \text{if } k \neq 0. \end{cases} \tag{22}$$

We can write

$$\boldsymbol{\mathcal{S}}_C(\boldsymbol{r}, x) = \sum_{k=-\infty}^{k=\infty} e^{ik\varphi}\, \tilde{\boldsymbol{\mathcal{S}}}_C^{(k)}(\boldsymbol{r}, x), \tag{23}$$

where

$$\tilde{\boldsymbol{\mathcal{S}}}_C^{(k)}(\boldsymbol{r}, x) = \delta_{k0}\boldsymbol{\mathcal{S}}_C(\boldsymbol{r}, x). \tag{24}$$

Substituting Equation (18) into Equation (11) and using Equations (24) and (9) we get

$$\boldsymbol{\mathcal{S}}(\boldsymbol{r}, \boldsymbol{\Omega}, x) = \sum_{k=-\infty}^{k=\infty} e^{ik\varphi}\, \tilde{\boldsymbol{\mathcal{S}}}^{(k)}(\boldsymbol{r}, \theta, x), \tag{25}$$

where

$$\tilde{\boldsymbol{\mathcal{S}}}^{(k)}(\boldsymbol{r}, \theta, x) = p_x\tilde{\boldsymbol{\mathcal{S}}}_l^{(k)}(\boldsymbol{r}, \theta, x) + (1 - p_x)\tilde{\boldsymbol{\mathcal{S}}}_C^{(k)}(\boldsymbol{r}, x), \tag{26}$$

with

$$\begin{aligned} \tilde{\boldsymbol{\mathcal{S}}}_l^{(k)}(\boldsymbol{r}, \theta, x) = \tilde{\boldsymbol{G}}^{(k)}(\boldsymbol{r}) + \frac{1}{\phi(x)}\int_{-\infty}^{+\infty} dx' \\ \times \oint \frac{d\boldsymbol{\Omega}'}{4\pi}\hat{W}\big\{\hat{M}_{\rm II}(\boldsymbol{B}, x, x')\tilde{r}_{\rm II}^{(k)}(x, x', \theta, \boldsymbol{\Omega}') \\ + \hat{M}_{\rm III}(\boldsymbol{B}, x, x')\tilde{r}_{\rm III}^{(k)}(x, x', \theta, \boldsymbol{\Omega}')\big\} \\ \times \hat{\Psi}(\boldsymbol{\Omega}')\boldsymbol{\mathcal{I}}(\boldsymbol{r}, \boldsymbol{\Omega}', x'). \end{aligned} \tag{27}$$

Substituting Equation (27) into Equation (14) we get

$$\boldsymbol{\mathcal{I}}(\boldsymbol{r}, \boldsymbol{\Omega}, x) = \sum_{k=-\infty}^{k=\infty} e^{ik\varphi}\, \tilde{\boldsymbol{\mathcal{I}}}^{(k)}(\boldsymbol{r}, \boldsymbol{\Omega}, x), \tag{28}$$

where

$$\begin{aligned} \tilde{\boldsymbol{\mathcal{I}}}^{(k)}(\boldsymbol{r}, \boldsymbol{\Omega}, x) = \tilde{\boldsymbol{\mathcal{I}}}^{(k)}(\boldsymbol{r}_0, \boldsymbol{\Omega}, x)e^{-\tau_{x,\max}} \\ + \int_0^{\tau_{x,\max}} e^{-\tau_x'(\boldsymbol{r}')}\tilde{\boldsymbol{\mathcal{S}}}^{(k)}(\boldsymbol{r}', \theta, x)\, d\tau_x'(\boldsymbol{r}'), \end{aligned} \tag{29}$$

with

$$\tilde{\boldsymbol{\mathcal{I}}}^{(k)}(\boldsymbol{r}_0, \boldsymbol{\Omega}, x) = \delta_{k0}\boldsymbol{\mathcal{I}}(\boldsymbol{r}_0, \boldsymbol{\Omega}, x). \tag{30}$$

Here, $\tilde{\boldsymbol{\mathcal{S}}}^{(k)}$ depends only on $\boldsymbol{r}'$ but not the variable of integration $\tau_x'(\boldsymbol{r}')$ which is measured along a given ray determined by the direction $\boldsymbol{\Omega}$. Substituting Equation (29) into Equation (27) we obtain

$$\begin{aligned} \tilde{\boldsymbol{\mathcal{S}}}_l^{(k)}(\boldsymbol{r}, \theta, x) = \tilde{\boldsymbol{G}}^{(k)}(\boldsymbol{r}) + \frac{1}{\phi(x)}\int_{-\infty}^{+\infty} dx' \\ \times \oint \frac{d\boldsymbol{\Omega}'}{4\pi}\hat{W}\big\{\hat{M}_{\rm II}(\boldsymbol{B}, x, x')\tilde{r}_{\rm II}^{(k)}(x, x', \theta, \boldsymbol{\Omega}') \\ + \hat{M}_{\rm III}(\boldsymbol{B}, x, x')\tilde{r}_{\rm III}^{(k)}(x, x', \theta, \boldsymbol{\Omega}')\big\}\hat{\Psi}(\boldsymbol{\Omega}') \\ \times \sum_{k'=-\infty}^{k'=+\infty} e^{ik'\varphi'}\tilde{\boldsymbol{\mathcal{I}}}^{(k')}(\boldsymbol{r}, \boldsymbol{\Omega}', x'). \end{aligned} \tag{31}$$

Now from Equations (25) and (28) and Equation (8) it is straightforward to show that the Fourier coefficients $\tilde{\boldsymbol{\mathcal{S}}}^{(k)}$ and $\tilde{\boldsymbol{\mathcal{I}}}^{(k)}$ satisfy a transfer equation of the form

$$-\frac{1}{\kappa_{\rm tot}(\boldsymbol{r}, x)}\boldsymbol{\Omega}\cdot\boldsymbol{\nabla}\tilde{\boldsymbol{\mathcal{I}}}^{(k)}(\boldsymbol{r}, \boldsymbol{\Omega}, x) = [\tilde{\boldsymbol{\mathcal{I}}}^{(k)}(\boldsymbol{r}, \boldsymbol{\Omega}, x) - \tilde{\boldsymbol{\mathcal{S}}}^{(k)}(\boldsymbol{r}, \theta, x)]. \tag{32}$$

This proves the theorem. Equation (18) represents the Fourier series expansion of the angle-dependent redistribution functions $r_{\rm II,III}(x, x', \boldsymbol{\Omega}, \boldsymbol{\Omega}')$. The expansion is with respect to the azimuth φ of the scattered ray. In this respect, our expansion method differs from those used in Domke & Hubeny (1988), HF09, HF10, and Sampoorna et al. (2011), all of whom perform expansion with respect to $\varphi - \varphi'$, where φ' is the incident ray azimuth. The expansion used by these authors naturally leads to axisymmetry of the Fourier components $\tilde{\boldsymbol{\mathcal{I}}}^{(k)}$, because of the 1D planar geometry assumed by them. In a multi-D geometry, the expansion with respect to $\varphi - \varphi'$ does not provide any advantage. In fact, $\tilde{\boldsymbol{\mathcal{I}}}^{(k)}$ continue to depend on φ due to finiteness of the coordinate axes X and/or Y in the multi-D geometry, under expansions either with respect to φ or $\varphi - \varphi'$. The Fourier expansion of $\boldsymbol{\mathcal{S}}$ in terms of φ (or $\varphi - \varphi'$) leads to axisymmetric $\tilde{\boldsymbol{\mathcal{S}}}^{(k)}$ in 1D as well as multi-D geometries. Thus, both the approaches are equivalent.

4.1. *Symmetry Properties of the Irreducible Fourier Coefficients*

From Equation (19) it is easy to show that the components $\tilde{r}_{\rm II,III}^{(k)}$ satisfy the conjugation property

$$\tilde{r}_{\rm II,III}^{(k)} = \big(\tilde{r}_{\rm II,III}^{(k)}\big)^*. \tag{33}$$

In other words, the real and imaginary parts of $\tilde{r}_{\rm II,III}^{(k)}$ are respectively symmetric and anti-symmetric about $k = 0$.

Using Equation (33) we can rewrite Equation (18) as

$$\begin{aligned} r_{\rm II,III}(x, x', \boldsymbol{\Omega}, \boldsymbol{\Omega}') = \tilde{r}_{\rm II,III}^{(0)}(x, x', \theta, \boldsymbol{\Omega}') \\ + \sum_{k=1}^{k=\infty}\big\{e^{-ik\varphi}\,\tilde{r}_{\rm II,III}^{(-k)}(x, x', \theta, \boldsymbol{\Omega}') \\ + e^{ik\varphi}\,\tilde{r}_{\rm II,III}^{(k)}(x, x', \theta, \boldsymbol{\Omega}')\big\} \end{aligned} \tag{34}$$

or

$$r_{\rm II,III}(x, x', \boldsymbol{\Omega}, \boldsymbol{\Omega}') = \sum_{k=0}^{k=\infty}(2 - \delta_{k0})e^{ik\varphi}\,\tilde{r}_{\rm II,III}^{(k)}(x, x', \theta, \boldsymbol{\Omega}'). \tag{35}$$

In Equation (35), the Fourier series constitutes only the terms with $k \geqslant 0$. This is useful in practical applications. With this simplification, we can show, following the steps similar to those given in Section 4, that Equation (16) now becomes

$$\begin{aligned} \boldsymbol{\mathcal{S}}(\boldsymbol{r}, \boldsymbol{\Omega}, x) = \sum_{k=0}^{k=\infty} e^{ik\varphi}(2 - \delta_{k0})\tilde{\boldsymbol{\mathcal{S}}}^{(k)}(\boldsymbol{r}, \theta, x), \\ \boldsymbol{\mathcal{I}}(\boldsymbol{r}, \boldsymbol{\Omega}, x) = \sum_{k=0}^{k=\infty} e^{ik\varphi}(2 - \delta_{k0})\tilde{\boldsymbol{\mathcal{I}}}^{(k)}(\boldsymbol{r}, \boldsymbol{\Omega}, x), \end{aligned} \tag{36}$$

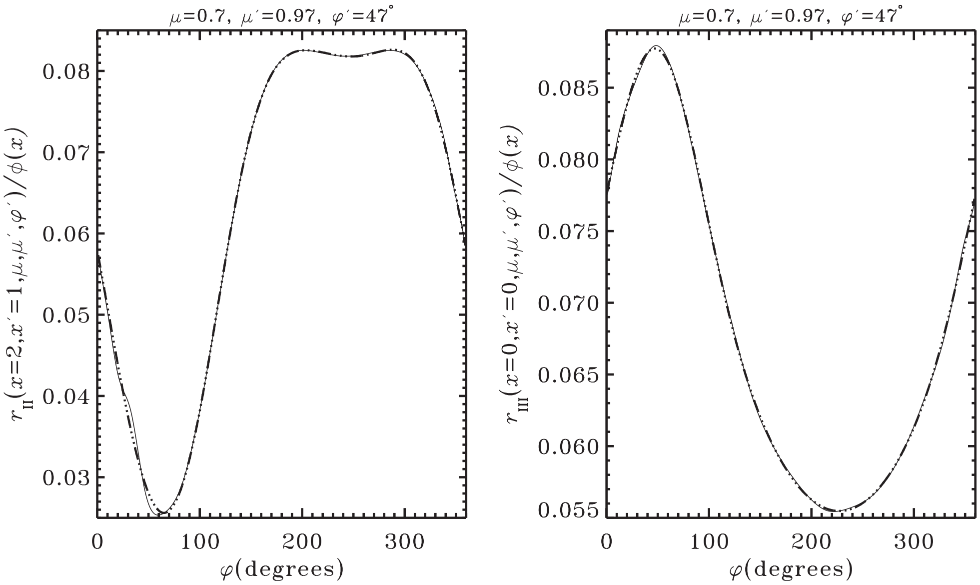

Figure 2. Comparison of the exact (solid lines) and Fourier expansion (dash-triple-dotted lines) of $r_{\rm II}$ and $r_{\rm III}$ functions with five terms retained in the series (Equation (35)).

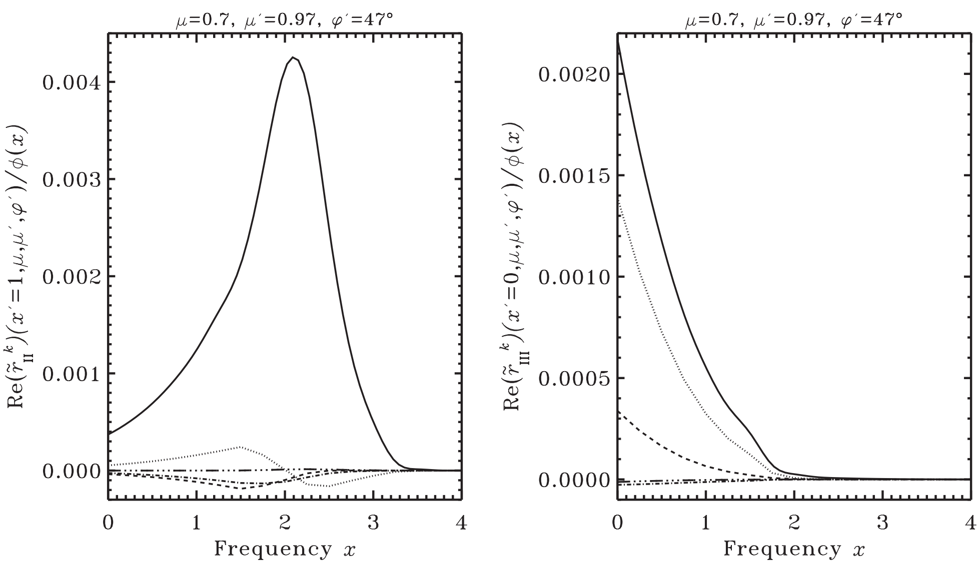

Figure 3. Frequency dependence of real parts of $\tilde{r}^{(k)}_{\rm II,III}(x, x', \theta, \boldsymbol{\Omega'})$. Solid, dotted, dashed, dot-dashed, and dash-triple-dotted lines correspond, respectively, to $k = 0$, $k = 1$, $k = 2$, $k = 3$, and $k = 4$.

where

$$\tilde{\boldsymbol{\mathcal{S}}}^{(k)}(\boldsymbol{r}, \theta, x) = p_x \tilde{\boldsymbol{\mathcal{S}}}^{(k)}_l(\boldsymbol{r}, \theta, x) + (1 - p_x)\tilde{\boldsymbol{\mathcal{S}}}^{(k)}_C(\boldsymbol{r}, x), \quad (37)$$

with

$$\tilde{\boldsymbol{\mathcal{S}}}^{(k)}_C(\boldsymbol{r}, x) = \delta_{k0}\boldsymbol{\mathcal{S}}_C(\boldsymbol{r}, x) \quad (38)$$

and

$$\begin{aligned}\tilde{\boldsymbol{\mathcal{S}}}^{(k)}_l(\boldsymbol{r}, \theta, x) = {} & \tilde{\boldsymbol{G}}^{(k)}(\boldsymbol{r}) + \frac{1}{\phi(x)} \int_{-\infty}^{+\infty} dx' \\ & \times \oint \frac{d\boldsymbol{\Omega}'}{4\pi} \hat{W} \Big\{ \hat{M}_{\rm II}(\boldsymbol{B}, x, x')\tilde{r}^{(k)}_{\rm II}(x, x', \theta, \boldsymbol{\Omega}') \\ & + \hat{M}_{\rm III}(\boldsymbol{B}, x, x')\tilde{r}^{(k)}_{\rm III}(x, x', \theta, \boldsymbol{\Omega}')\Big\}\hat{\Psi}(\boldsymbol{\Omega}') \\ & \times \sum_{k'=0}^{k'=+\infty} e^{ik'\varphi'}(2 - \delta_{k'0})\tilde{\boldsymbol{\mathcal{I}}}^{(k')}(\boldsymbol{r}, \boldsymbol{\Omega}', x'). \quad (39)\end{aligned}$$

The components of $\tilde{\boldsymbol{\mathcal{S}}}^{(k)}$ and $\tilde{\boldsymbol{\mathcal{I}}}^{(k)}$ in general form countably infinite sets.[1] We have verified that for practical applications it is sufficient to work with five terms in the Fourier series ($k \in [0, +4]$). Figure 2 shows a plot of the $r_{\rm II,III}$ functions computed using an exact method (as in Nagendra et al. 2002), and those computed using Equation (35) with $k \in [0, +4]$, namely keeping only the five dominant components in the series expansion. A similar comparison of the exact and series expansion methods for $r_{\rm II}$ is presented by Domke & Hubeny (1988), who also show that five dominant components are sufficient to accurately represent the angle-dependent $r_{\rm II}$ function.

In Figures 3 and 4 we study the frequency dependence of the real and imaginary parts of $\tilde{r}^{(k)}_{\rm II,III}(x, x', \theta, \boldsymbol{\Omega'})$ for a given incident frequency point ($x' = 2$ for $\tilde{r}^{(k)}_{\rm II}$ and $x' = 0$ for $\tilde{r}^{(k)}_{\rm III}$). We show

[1] If a set has a one-to-one correspondence with the set of integers, it is called a countably infinite set.

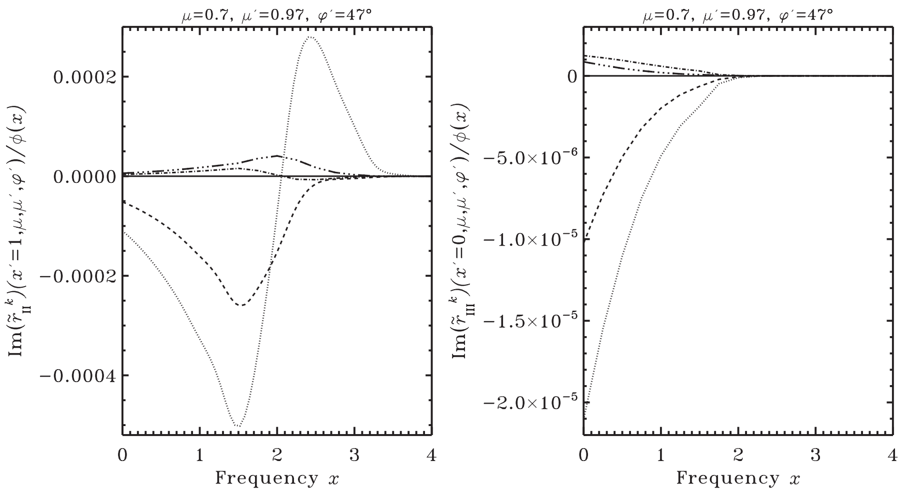

Figure 4. Frequency dependence of imaginary parts of $\tilde{r}^{(k)}_{\rm II,III}(x, x', \theta, \mathbf{\Omega}')$. Solid, dotted, dashed, dot-dashed, and dash-triple-dotted lines correspond, respectively, to $k = 0$, $k = 1$, $k = 2$, $k = 3$, and $k = 4$.

the behavior of five ($k = 0, 1, 2, 3, 4$) Fourier components. Note that $\tilde{r}^{(0)}_{\rm II,III}$ are real quantities.

Equations (29) and (32) together with Equations (37)–(39) can be solved using an iterative method. In a subsequent paper, we develop a fast iterative method (pre-BiCG-STAB) and present the solutions of polarized RT in multi-D geometry including Hanle effect with angle-dependent PRD.

After solving for $\tilde{\boldsymbol{\mathcal{S}}}^{(k)}$ and $\tilde{\boldsymbol{\mathcal{I}}}^{(k)}$, we can construct $\boldsymbol{\mathcal{S}}$ and $\boldsymbol{\mathcal{I}}$ using Equation (36). Since $\boldsymbol{\mathcal{S}}$ and $\boldsymbol{\mathcal{I}}$ are real quantities, these expansions reduce to the following simpler forms:

$$\boldsymbol{\mathcal{S}}(\boldsymbol{r}, \mathbf{\Omega}, x) = \sum_{k=0}^{k=\infty}(2 - \delta_{k0})\{\cos(k\varphi)\mathcal{R}e\{\tilde{\boldsymbol{\mathcal{S}}}^{(k)}(\boldsymbol{r}, \theta, x)\} - \sin(k\varphi)\mathcal{I}m\{\tilde{\boldsymbol{\mathcal{S}}}^{(k)}(\boldsymbol{r}, \theta, x)\}\}, \tag{40}$$

and

$$\boldsymbol{\mathcal{I}}(\boldsymbol{r}, \mathbf{\Omega}, x) = \sum_{k=0}^{k=\infty}(2 - \delta_{k0})\{\cos(k\varphi)\mathcal{R}e\{\tilde{\boldsymbol{\mathcal{I}}}^{(k)}(\boldsymbol{r}, \mathbf{\Omega}, x)\} - \sin(k\varphi)\mathcal{I}m\{\tilde{\boldsymbol{\mathcal{I}}}^{(k)}(\boldsymbol{r}, \mathbf{\Omega}, x)\}\}, \tag{41}$$

where $\boldsymbol{\mathcal{S}} = (S^0_0, S^2_0, S^{2,\rm x}_1, S^{2,\rm y}_1, S^{2,\rm x}_2, S^{2,\rm y}_2)^T$ and $\boldsymbol{\mathcal{I}} = (I^0_0, I^2_0, I^{2,\rm x}_1, I^{2,\rm y}_1, I^{2,\rm x}_2, I^{2,\rm y}_2)^T$.

Once we obtain $\boldsymbol{\mathcal{S}}$ and $\boldsymbol{\mathcal{I}}$, the Stokes source vector and Stokes intensity vector can be deduced using the following formulae (see Appendix B of HF07 and also Paper I):

$$I(\boldsymbol{r}, \mathbf{\Omega}, x) = I^0_0 + \frac{1}{2\sqrt{2}}(3\cos^2\theta - 1)I^2_0 - \sqrt{3}\cos\theta\sin\theta\left(I^{2,\rm x}_1\cos\varphi - I^{2,\rm y}_1\sin\varphi\right) + \frac{\sqrt{3}}{2}(1 - \cos^2\theta)\left(I^{2,\rm x}_2\cos 2\varphi - I^{2,\rm y}_2\sin 2\varphi\right), \tag{42}$$

$$Q(\boldsymbol{r}, \mathbf{\Omega}, x) = -\frac{3}{2\sqrt{2}}(1 - \cos^2\theta)I^2_0 - \sqrt{3}\cos\theta\sin\theta\left(I^{2,\rm x}_1\cos\varphi - I^{2,\rm y}_1\sin\varphi\right) - \frac{\sqrt{3}}{2}(1 + \cos^2\theta)\left(I^{2,\rm x}_2\cos 2\varphi - I^{2,\rm y}_2\sin 2\varphi\right), \tag{43}$$

$$U(\boldsymbol{r}, \mathbf{\Omega}, x) = \sqrt{3}\sin\theta\left(I^{2,\rm x}_1\sin\varphi + I^{2,\rm y}_1\cos\varphi\right) + \sqrt{3}\cos\theta\left(I^{2,\rm x}_2\sin 2\varphi + I^{2,\rm y}_2\cos 2\varphi\right). \tag{44}$$

The quantities I^0_0, I^2_0, $I^{2,\rm x}_1$, $I^{2,\rm y}_1$, $I^{2,\rm x}_2$, and $I^{2,\rm y}_2$ also depend on $\boldsymbol{r}$, $\mathbf{\Omega}$, and x. Similar formulae can also be used to deduce $\boldsymbol{S}$ from $\boldsymbol{\mathcal{S}}$.

5. NUMERICAL CONSIDERATIONS

The proposed Fourier series expansion (or Fourier decomposition) technique to solve multi-D RT problems with angle-dependent PRD functions essentially transforms the given problem in the (θ, φ) space (see Section 3) into the (θ, k) space (see Section 4). Let n_φ denote the number of azimuths (φ) used in the computations and n_k the maximum number of terms retained in the Fourier series expansions. In the (θ, φ) space, the source terms $\boldsymbol{\mathcal{S}}$ depend on n_φ, whereas in the (θ, k) space the source terms $\tilde{\mathcal{S}}^{(k)}$ depend on n_k. In Figure 2 we have demonstrated that it is sufficient to work with $n_k = 5$ (i.e., $k \in [0, 4]$), whereas for 2D RT problems it is necessary to use $n_\varphi = 8$, 16, 24, or 32, depending upon the accuracy requirements of the problem. Since n_k is always smaller than n_φ, the computational cost is reduced when we work in the (θ, k) space.

In addition to the computation of $r_{\rm II,III}(x, x', \mathbf{\Omega}, \mathbf{\Omega}')$ functions, we need to compute $\tilde{r}^{(k)}_{\rm II,III}(x, x', \theta, \mathbf{\Omega}')$ in the (θ, k) space. This additional computation does not require much CPU time. Moreover, if we can fix the number of angles and frequency points to be used in the computations, it is sufficient to compute these functions only once, which can be written in a file. In subsequent transfer computations, these data can simply be read from the archival file.

To demonstrate these advantages, we have compared the CPU time requirements for the two methods, one which uses the (θ, φ) space and the other which uses the (θ, k) space. Both approaches use Pre-BiCG-STAB as the iterative method to solve the 2D transfer problem. We find that with $n_\varphi = 32$, the CPU time required to solve a given problem in the (θ, k) space is seven times less than that required in the (θ, φ) space. For practical problems requiring more azimuthal angles, the advantage of using a Fourier decomposition technique is much larger.

To demonstrate the correctness of the proposed Fourier decomposition technique for the multi-D transfer, we consider a test RT problem in the 2D medium. A complete study of

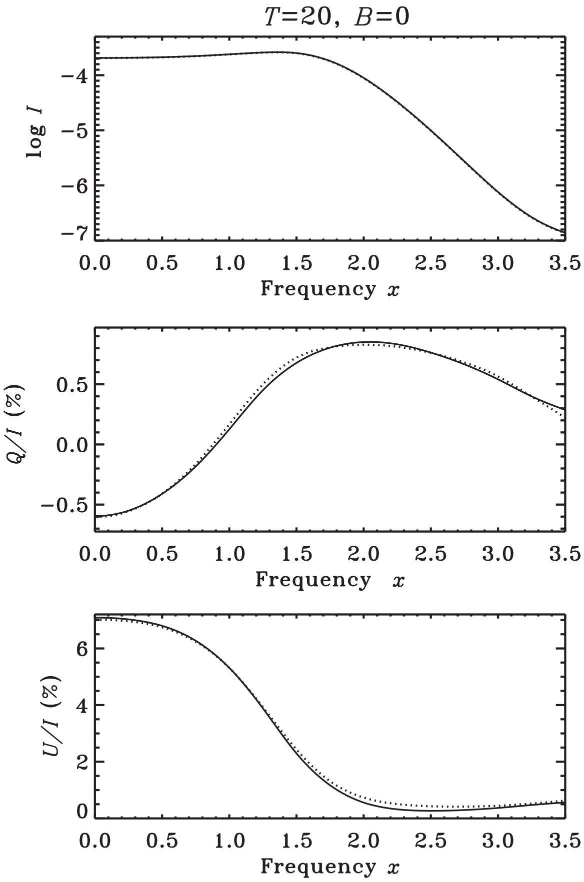

Figure 5. Emergent, spatially averaged I, Q/I, U/I profiles computed for a test 2D RT problem with angle-dependent PRD using two methods, one which uses (θ, k) space (solid lines) and the other which uses the (θ, φ) space (dotted lines). Both the approaches use the Pre-BiCG-STAB as the iterative method. Both methods produce nearly identical results, proving the correctness of the proposed Fourier decomposition technique for angle-dependent PRD problems in multi-D RT. The results are plotted for $\mu = 0.1$ and $\varphi = 27°$. The details and other model parameters are given in Section 5.

the solutions of 2D RT problems with angle-dependent PRD will be taken up in a forthcoming paper. Figure 5 shows the emergent, spatially averaged Stokes profiles formed in a 2D medium, computed using the two methods mentioned above. The model parameters are the total optical thickness in two directions, namely $T_Y = T_Z = T = 20$, the elastic and inelastic collision rates, respectively, are $\Gamma_E/\Gamma_R = 10^{-4}, \Gamma_I/\Gamma_R = 10^{-4}$, and the damping parameter of the Voigt profile is $a = 2 \times 10^{-3}$. We consider the pure line case ($\kappa_c = 0$). The internal thermal sources are taken as constant (the Planck function $B_\nu = 1$). The medium is assumed to be self-emitting (no incident radiation on the boundaries). We consider the case of zero magnetic field. The branching ratios for this choice of model parameters are $(\alpha, \beta^{(0)}, \beta^{(2)}) = (1, 1, 1)$. These branching ratios correspond to a PRD scattering that uses only the $\tilde{r}^{(k)}_{\mathrm{II}}(x, x', \theta, \mathbf{\Omega}')$ function. We use a logarithmic frequency grid with $x_{\max} = 3.5$ and a logarithmic depth grid in the Y- and Z-directions of the 2D medium. We have used a three-point Gaussian μ-quadrature and a 32-point Gaussian φ-quadrature. In Figure 5 we show the results computed at $\mu = 0.1$ and $\varphi = 27°$. The fact that both the methods give nearly identical results proves the correctness of the proposed Fourier decomposition technique for multi-D RT.

6. CONCLUSIONS

In this paper, we formulate the polarized RT equation in multi-D media that includes angle-dependent PRD and the Hanle effect. We propose a method for decomposition of the Stokes source vector and Stokes intensity vector in terms of irreducible Fourier components $\tilde{\mathcal{S}}^{(k)}$ and $\tilde{\mathcal{I}}^{(k)}$, using a combination of the decomposition of the scattering phase matrices in terms of irreducible spherical tensors $\mathcal{T}^K_Q$ and the Fourier series expansions of angle-dependent PRD functions. We also establish that the irreducible Fourier components $\tilde{\mathcal{S}}^{(k)}$ and $\tilde{\mathcal{I}}^{(k)}$ satisfy a simple transfer equation, which can be solved by any iterative method such as an ALI or a Bi-Conjugate Gradient-type projection method.

We thank Professor H. Frisch for helpful comments/suggestions that helped to improve the manuscript. We also thank Dr. Sampoorna for useful discussions.

REFERENCES

Adam, J. 1990, A&A, 240, 541
Anusha, L. S., & Nagendra, K. N. 2011a, ApJ, 726, 6 (Paper I)
Anusha, L. S., & Nagendra, K. N. 2011b, ApJ, 738, 116 (Paper III)
Anusha, L. S., Nagendra, K. N., & Paletou, F. 2011, ApJ, 726, 96 (Paper II)
Bommier, V. 1997a, A&A, 328, 706
Bommier, V. 1997b, A&A, 328, 726
Chandrasekhar, S. 1946, ApJ, 103, 351
Chandrasekhar, S. 1960, Radiative Transfer (New York: Dover)
Dittmann, O. J. 1999, in Solar Polarization 2, ed. K. N. Nagendra & J. O. Stenflo (Boston, MA: Kluwer), 201
Domke, H., & Hubeny, I. 1988, ApJ, 334, 527
Dumont, S., Omont, A., Pecker, J. C., & Rees, D. E. 1977, A&A, 54, 675
Faurobert, M. 1987, A&A, 178, 269
Faurobert, M. 1988, A&A, 194, 268
Faurobert-Scholl, M. 1991, A&A, 246, 469
Frisch, H. 2007, A&A, 476, 665 (HF07)
Frisch, H. 2009, in ASP Conf. Ser. 405, Solar Polarization 5, ed. S. V. Berdyugina, K. N. Nagendra, & R. Ramelli (San Francisco, CA: ASP), 87 (HF09)
Frisch, H. 2010, A&A, 522, A41
Hamilton, D. R. 1947, ApJ, 106, 457
Hummer, D. G. 1962, MNRAS, 125, 21
Landi Degl'Innocenti, E., Bommier, V., & Sahal-Bréchot, S. 1987, A&A, 186, 335
Landi Degl'Innocenti, E., & Landolfi, M. 2004, Polarization in Spectral Lines (Dordrecht: Kluwer)
Landi Degl'Innocenti, M., & Landi Degl'Innocenti, E. 1988, A&A, 192, 374
Manso Sainz, R., & Trujillo Bueno, J. 1999, in Solar Polarization 2, ed. K. N. Nagendra & J. O. Stenflo (Boston, MA: Kluwer), 143
McKenna, S. J. 1985, Ap&SS, 108, 31
Mihalas, D., Auer, L. H., & Mihalas, B. R. 1978, ApJ, 220, 1001
Nagendra, K. N. 1986, PhD thesis, Bangalore Univ.
Nagendra, K. N. 1994, ApJ, 432, 274
Nagendra, K. N., Frisch, H., & Faurobert, M. 2002, A&A, 395, 305
Nagendra, K. N., Frisch, H., & Fluri, D. M. 2003, in ASP Conf. Ser. 307, Solar Polarization 3, ed. J. Trujillo Bueno & J. Sánchez Almeida (San Francisco, CA: ASP), 227
Nagendra, K. N., & Sampoorna, M. 2011, A&A, submitted
Omont, A., Smith, E. W., & Cooper, J. 1972, ApJ, 175, 185
Omont, A., Smith, E. W., & Cooper, J. 1973, ApJ, 182, 283
Paletou, F., Bommier, V., & Faurobert-Scholl, M. 1999, in Solar Polarization 2, ed. K. N. Nagendra & J. O. Stenflo (Boston, MA: Kluwer), 189
Pomraning, G. C. 1973, The Equations of Radiation Hydrodynamics (Oxford: Pergamon Press)
Rees, D. E. 1978, PASJ, 30, 455
Rees, D. E., & Saliba, G. J. 1982, A&A, 115, 1
Sampoorna, M. 2011, A&A, 532, A52
Sampoorna, M., Nagendra, K. N., & Frisch, H. 2011, A&A, 527, A89
Sampoorna, M., Nagendra, K. N., & Stenflo, J. O. 2008, ApJ, 679, 889
Stenflo, J. O. 1978, A&A, 66, 241